
OsHV-1 countermeasures to the Pacific oyster's anti-viral response

Green Timothy^{1,2,*}, Rolland Jean-Luc³, Vergnes Agnes³, Raftos David^{1,2}, Montagnani Caroline³

¹ Department of Biological Sciences, Macquarie University, NSW 2109, Australia

² Sydney Institute of Marine Science, Chowder Bay Road, Mosman, NSW 2088, Australia

³ IFREMER, IHPE, UMR 5244, Univ. Perpignan Via Domitia, CNRS, Univ. Montpellier, F-34095, Montpellier, France

* Corresponding author : Timothy J. Green, email address : tim.green@mq.edu.au

Abstract :

The host-pathogen interactions between the Pacific oyster (*Crassostrea gigas*) and Ostreid herpesvirus type 1 (OsHV-1) are poorly characterised. Herpesviruses are a group of large, DNA viruses that are known to encode gene products that subvert their host's antiviral response. It is likely that OsHV-1 has also evolved similar strategies as its genome encodes genes with high homology to *C. gigas* inhibitors of apoptosis (IAPs) and an interferon-stimulated gene (termed CH25H). The first objective of this study was to simultaneously investigate the expression of *C. gigas* and OsHV-1 genes that share high sequence homology during an acute infection. Comparison of apoptosis-related genes revealed that components of the extrinsic apoptosis pathway (TNF) were induced in response to OsHV-1 infection, but we failed to observe evidence of apoptosis using a combination of biochemical and molecular assays. IAPs encoded by OsHV-1 were highly expressed during the acute stage of infection and may explain why we didn't observe evidence of apoptosis. However, *C. gigas* must have an alternative mechanism to apoptosis for clearing OsHV-1 from infected gill cells as we observed a reduction in viral DNA between 27 and 54 h post-infection. The reduction of viral DNA in *C. gigas* gill cells occurred after the up-regulation of interferon-stimulated genes (viperin, PKR, ADAR). In a second objective, we manipulated the host's anti-viral response by injecting *C. gigas* with a small dose of poly I:C at the time of OsHV-1 infection. This small dose of poly I:C was unable to induce transcription of known antiviral effectors (ISGs), but these oysters were still capable of inhibiting OsHV-1 replication. This result suggests dsRNA induces an anti-viral response that is additional to the IFN-like pathway.

Highlights

► Components of the oyster apoptosis pathway (TNF) are induced in response to OsHV-1. ► OsHV-1 genome encodes multiple inhibitors of apoptosis, which are highly expressed during the acute infection. ► Results from biochemical assays suggest apoptosis isn't occurring in response to OsHV-1 infection, suggesting the virus may regulate apoptosis. ► Host ISG expression was not activated in oyster's injected with a low concentration of poly I:C. ► Oyster's simultaneously injected with a low concentration of poly I:C and OsHV-1 were capable of inhibiting virus replication, suggesting dsRNA induces an anti-viral response that is additional to the IFN-like pathway.

Keywords : *Crassostrea*, anti-viral response, apoptosis, interferon-like, poly I:C

57 1.0 Introduction

58 Anti-viral immunity in molluscs is poorly understood [1, 2]. Most of our
59 understanding of invertebrate anti-viral immunity stems from model systems, such as
60 *Drosophila melanogaster*, mosquitoes (*Anopheles gambiae* and *Aedes aegypti*) and
61 *Caenorhabditis elegans* [3-6]. RNA interference (RNAi) is the central part of the innate
62 immune response of these model invertebrate species [4, 6, 7]. Additional anti-viral
63 responses utilised by *Drosophila* and mosquitoes include programmed cell death (*i.e.*
64 apoptosis and autophagy) [5, 8] and a transcriptional response involving a set of genes
65 that inhibit virus replication [9, 10]. These anti-viral responses of model-invertebrates
66 are quite different to the vertebrate innate immune response to viral infection.
67 Vertebrate cells rarely utilise the RNAi-mediated anti-viral response [11]. Instead, the
68 vertebrate innate immune system relies on recognising virus-derived nucleic acids
69 through pathogen recognition receptors (*i.e.* Toll-like receptors, RIG-like receptors,
70 cGAS) [12]. Engagement of these receptors activates the interferon (IFN)-pathway,
71 which is an extremely powerful anti-viral response [12]. IFNs exert their anti-viral
72 response by binding their cognate receptors on all nucleated cells, signal through the
73 JAK-STAT pathway, and transcriptionally induce hundreds of IFN-stimulated genes
74 (ISGs) that are collectively capable of controlling most, if not all, virus infections [12,
75 13]. It was believed invertebrates lacked anti-viral systems homologous to the
76 vertebrate IFN-response because model invertebrates (*Drosophila*, mosquitoes and
77 *Caenorhabditis*) genomes do not encode IFN-cytokines or ISGs [14].

78 New evidence suggests the IFN-pathway evolved in the common metazoan
79 ancestor with interferon-related genes present in the genomes of animals belonging to
80 the phylums of Mollusca [2, 15], Cnidaria [16] and Porifera [17, 18]. Analysis of model
81 invertebrate genomes reveal they have undergone substantial gene loss [19, 20], which
82 appears to also include genes related to the IFN-pathway. The genome of Pacific oyster
83 (*Crassostrea gigas*) encodes many ISGs that are up-regulated in response to Ostreid
84 herpesvirus type 1 (OsHV-1) [15, 21-23]. The expression of these ISGs can be induced
85 by injecting *C. gigas* with virus-associated nucleic acids (poly I:C) [24, 25] and this
86 response is protective against OsHV-1 infection [22]. Programmed cell death involving
87 autophagy is also involved in the *C. gigas* response to experimental infection with OsHV-
88 1 [26]. Autophagy is induced in the mantle tissue of *C. gigas* in response to OsHV-1
89 infection and survival assays incorporating known inhibitors of autophagy have

90 demonstrated that this anti-viral response has a protective role against OsHV-1 [26].
91 However, it is unknown if other evolutionally conserved immune responses present in
92 vertebrates and arthropods, such as RNAi and apoptosis also contribute to molluscan
93 anti-viral immunity.

94 The incomplete understanding of anti-viral immunity in molluscs is hampering
95 effective management of emerging viral diseases affecting aquaculture production of
96 marine bivalves [27, 28] and gastropods [29, 30], mainly caused by viruses belonging to
97 the Herpesvirales order [28, 31-33]. Herpesviruses constitute a large family of
98 enveloped, double-stranded DNA viruses that are responsible for many human and
99 animal diseases. The genomes of mammalian herpesviruses encode many gene
100 products that subvert the host's anti-viral response and exploit their host's cellular
101 machinery for their own benefit [reviewed by 34, 35, 36]. For example, the genome of
102 Human herpesvirus-8 (HHV-8) contains 86 genes, of which at least 22 encode proteins
103 that are immunomodulatory [34]. Since the IFN-response is the major innate anti-viral
104 response of humans, HHV-8 encodes at least seven proteins that suppress the IFN-
105 response [reviewed by 34]. It is likely that molluscan herpesviruses have also
106 developed similar strategies to evade their host's innate immune response and persist.
107 Identifying these strategies could provide insight into the major anti-viral pathways of
108 molluscs.

109 The genome of Ostreid herpesvirus type 1 (OsHV-1) contains 124 open reading
110 frames (ORFs) and eight of these ORFs encode proteins with high homology (E-value <
111 1×10^{-5} , Score >200) to proteins encoded by the genome of the Pacific oyster, *Crassostrea*
112 *gigas* [21]. These OsHV-1 ORFs include four inhibitors of apoptosis (ORF42, 87, 99,
113 106), two super-family type 2 helicases (ORF67, 115), ribonuclease reductase (ORF51),
114 and transmembrane protein with high homology to *C. gigas* cholesterol-25-hydroxylase
115 (ORF57) [33]. Vertebrate cholesterol-25-hydroxylase (CH25H) is an IFN-stimulated
116 enzyme that converts cholesterol to a soluble anti-viral factor, 25-hydroxycholesterol,
117 that suppresses viral growth by blocking membrane fusion between virus and cell [37].
118 These observations suggest that OsHV-1 has the potential to modulate the anti-viral
119 response of *C. gigas* by inhibiting apoptosis and interfering with ISGs. OsHV-1 also
120 appears to be able to modulate host DNA synthesis by encoding enzymes involved in
121 nucleotide biosynthesis (ribonuclease reductase) and DNA/RNA metabolism (SF2
122 Helicases)[38].

123 In this study, the first objective was to investigate OsHV-1 countermeasures to
124 the oyster's anti-viral response by simultaneously comparing mRNA expression levels
125 of *C. gigas* and OsHV-1 genes during an experimental infection. Genes investigated
126 include host and virus genes that share high homology (IAPs, CH25H, SF2 Helicases &
127 ribonucleotide reductase) and an additional set of host genes involved in the extrinsic
128 apoptotic pathway (TNF, TNF receptors, FADD and caspases). Apoptosis was also
129 quantified in gill tissue of *C. gigas* at discrete time-points using biochemical assays to
130 measure caspase-3/7 activity and localise apoptotic cells in histological sections. The
131 second objective of this study was to identify if oysters have anti-viral responses
132 induced by dsRNA that are additional to the already described IFN-like response [22,
133 25]. To achieve this second objective, we simultaneously injected *C. gigas* with OsHV-1
134 and a low concentration of poly I:C (1 mg.ml⁻¹). This concentration of poly I:C was
135 chosen because it is insufficient to induce ISG expression in *C. gigas*.

136

137 **2.0 Materials and Methods**

138 2.1 Animals and OsHV-1 inoculum

139 Pacific oysters (*Crassostrea gigas*) were produced at the IFREMER Oyster
140 Hatchery in Argenton, France. Oysters were grown-out in a biosecure nursery facility at
141 the IFREMER facility of Bouin (France) before being transferred to IFREMER's
142 Aquaculture Research Facility in Palavas-les-Flots (Laboratoire Aquaculture en
143 Languedoc Roussillon, LALR), France. At the time of experimentation, these oysters
144 were classified to be juveniles (age = 6 months, shell length = 38.8 ± 4.0 mm) and they
145 were entering the early stages of spermatogenesis as assessed by histology (results not
146 presented). These oysters were used for all experiments outlined in this manuscript.

147 An initial OsHV-1 homogenate was prepared according to Schikorski et al., [39]
148 from ten dead oyster spat collected during an OsHV-1 mortality event (summer 2014)
149 in Thau Lagoon, France. Dead spat were homogenised in 10-volumes of autoclaved
150 seawater. The oyster homogenate was clarified by centrifugation (1000 x g for 10 min,
151 4°C) before serial filtration (8.0, 0.45 & 0.22 µm). The OsHV-1 homogenate was
152 confirmed to be free of culturable bacteria by plating 100 µl of homogenate on marine
153 agar. Twenty-five juvenile oysters were injected with 50 µl of OsHV-1 homogenate in
154 the adductor muscle through a notch filed in the oyster shell. Another 20 juvenile
155 oysters were injected with 50 µl of autoclaved seawater (controls) and these two

156 groups were placed in separate aquariums with filtered-seawater (aerated, 22°C). At 3
157 days post injection, gill and mantle tissue from 4 moribund oysters (OsHV-1
158 homogenate) and 4 healthy oysters (seawater control) was excised using a sterile
159 scalpel blade. Tissue from moribund and healthy oysters was used to make a fresh
160 OsHV-1 and control homogenate as per the methods outlined above, respectively. The
161 OsHV-1 genome copy number of the OsHV-1 and control homogenate was estimated by
162 qPCR (see below) and these new homogenates were used for experimentation outlined
163 below.

164

165 2.2 Experimental conditions

166 Prior to experimentation, 240 oysters had a notch filed in the side of their shell
167 using an electric bench grinder to allow delivery of oyster homogenates and poly I:C.
168 Oysters were distributed to twelve aerated aquariums (22±1°C) containing 20 L of
169 filtered seawater (20 oysters per tank). Oysters were allowed to acclimatise to their
170 research aquaria for 24 h.

171 At time 0 h, oysters were injected with 100 µl of one of four treatments into the
172 adductor muscle using a 26-gauge needle attached to a multi-dispensing hand pipette.
173 There were three replicate aquariums for each treatment. The four treatments
174 consisted of (A) OsHV-1 homogenate, (B) OsHV-1 homogenate + poly I:C, (C) control
175 homogenate, and (D) control homogenate + poly I:C. The concentration of OsHV-1 DNA
176 in the virus homogenates was 5.98×10^4 viral DNA copies.µl⁻¹. Poly I:C (Sigma, cat
177 #P0913) was resuspended in the OsHV-1 and control homogenates to a final
178 concentration of 1 mg.ml⁻¹, which resulted in each oyster being injected with 100 µg of
179 poly I:C.

180 Two oysters were sampled from each aquarium at 0, 3, 9, 27 and 54 hours post-
181 injection. Cumulative mortality was assessed at 96 h for each treatment from the
182 remaining 10 oysters in each tank. Sampling consisted of shucking each individual
183 oyster and excising the gill tissue using a sterile scalpel blade. Gill tissue was
184 homogenised and divided into three sub-samples: two sub-samples were snap-frozen at
185 -80°C for RNA and DNA purification and the third sub-sample was resuspended in 250
186 µl of 0.01M phosphate buffered saline (PBS, Sigma cat #P3813) for caspase activity
187 assay and kept on ice. We chose to study the gill tissue because it is one of the main

188 tissue compartments for detecting OsHV-1 mRNAs by *in-situ* hybridisation [40]. The
189 remaining oyster tissue was fixed in Seawater Davidson's fixative [41].

190

191 2.3 Nucleic acid extraction and qPCR

192 Total RNA was purified from gill tissue samples using bead-beating (Retsch MM
193 400) and Trizol (Invitrogen, cat #15596-026) according to the manufacturers protocol.
194 DNA was purified from gill tissue using a standard phenol:chloroform purification.
195 Quantity and purity of nucleic acids was assessed by spectrophotometry (Thermo
196 Scientific, ND-1000). RNA and DNA were resuspended in sterile water to a final
197 concentration of 100 and 20 ng.µl⁻¹, respectively. First-strand synthesis was performed
198 on 500 ng of total RNA using 250 ng of random hexamer primers (Invitrogen, cat
199 #48190-011) and 200 units of M-MLV RT (Invitrogen, cat #28025-013). cDNA was
200 diluted ten-fold in sterile water prior to use.

201 The detection and quantification of OsHV-1 DNA was performed on individual
202 oysters according to Pepin and colleagues [42] using a LightCycler 480 Real-Time
203 Thermocycler (Roche). PCR reaction volumes were 6 µl containing LightCycler 480
204 SYBR Green I Master Mix (Roche), 100 nM of C9 and C10 primers [42] and 20 ng of DNA.
205 All PCR reactions were performed in duplicate and absolute quantification of OsHV-1
206 DNA copies were estimated from a standard curve of the C9/C10 amplification (R²=
207 0.990) product cloned into the pCR4-TOPO vector as per Green and Montagnani [22].
208 The linear dynamic range of the qPCR assay was assessed using ten-fold serial dilutions
209 of the TOPO-C9/C10 plasmid, which revealed the upper and lower quantifiable limits to
210 be 10⁹ to 10¹ copies per ng of total DNA, respectively. The quantifiable lower limit
211 measured in the current study is in agreement with Pepin and colleagues [42].

212 Host and virus gene expression was quantified in individual oysters using an
213 Echo® 525 Liquid Handler (Labcyte) and LightCycler 480 Real-Time Thermocycler
214 (Roche). PCR reaction volumes were 1.5 µl containing LightCycler 480 SYBR Green I
215 Master Mix (Roche), 0.5 nM of gene specific primers (Table 1) and 0.5 µl of cDNA in a
216 LightCycler 480 Real-Time thermocycler (Roche) using an initial denaturation (95°C for
217 5 min) followed by 40 cycles of denaturation (95°C, 10s), hybridisation (60°C, 20s) and
218 elongation (72°C, 25s). A subsequent melting temperature curve of the amplicon was
219 performed and expression of *C. gigas* target genes were normalised with eEF1α
220 reference gene [43].

221 OsHV-1 gene expression was reported as both quantitative and qualitative
222 values. No gene has yet been identified in the OsHV-1 genome that is uniformly
223 expressed at the same level in all samples [44-47]. This prevents calculations involving
224 a valid internal reference gene ($2^{\Delta Ct}$). Quantitative values for OsHV-1 gene expression
225 were therefore normalised according to the method outlined by Segarra et al., [46]
226 using the formula: $F = \text{Log}_{10} ((E+1)^{40-Ct}/N)$, where E is qPCR efficiency of each viral gene,
227 Ct (cycle threshold) corresponds to the PCR cycle number, N is the number of viral DNA
228 copies.ng⁻¹ of total DNA determine by absolute qPCR for each individual and Ct = 40 is
229 arbitrarily considered to 'no Ct' obtained by qPCR. Qualitative gene expression was
230 reported as raw values (crossing-point, Cp) and a sample was considered to contain
231 OsHV-1 RNA when the fluorescence of SYBR in the RTqPCR assay exceeded the
232 background fluorescent threshold of 0.1 RFU.

233

234 2.4 Histology & TUNEL assay

235 Oyster tissue fixed in Seawater Davidson's solution was dehydrated and
236 embedded in Paraplast® (Sigma, cat #A6330) using standard histological techniques.
237 Serial sections of 5 µm thickness were cut and one section was adhered to StarFrost®
238 hydrophilic slide (Waldemar Knittel) for hematoxylin-eosin staining, while the
239 companion section was adhered to a StarFrost® silane coated slide (Waldemar Knittel)
240 for TUNEL assay. Histological sections were pre-treated with 10 µg.ml⁻¹ of proteinase K
241 (Roche, cat #03 115 887 001) for 15 min before being analysed with the In Situ Cell
242 Death Detection Kit, TMR red (Roche Applied Science, cat #12 156 792 910). Controls
243 included the TUNEL reaction mixture without terminal transferase (negative control)
244 and histology sections treated with DNase I (positive control). Sections were
245 counterstained with 30 nM.ml⁻¹ 4',6-diamidino-2'-phenylindole dihydrochloride (Roche
246 Applied Science, cat #10236276001) for 5 min, and visualised with a fluorescent
247 compound microscope (Leica DM5500 B) equipped with standard red (N3 λex: 546/12
248 nm, λem: 600/40 nm; TMR red) and blue (A4 λex: 360/40 nm, λem: 470 nm; DAPI)
249 filter sets.

250

251 2.5 Caspase-3/7 activity assay

252 Apoptosis was quantified fluorimetrically from caspase-3/7 activity at 0, 27 and
253 54 hours post injection. Caspase activity was determined using the SensoLyte®

254 Homogenous AFC Caspase-3/7 Assay Kit (AnaSpec Inc. cat #AS-71114) according to
255 Rolland et al., [48]. Briefly, gill tissue (50 mg) was homogenised in 250 µl of PBS using a
256 Potter-Elvehjem glass pestle and tube. In duplicate, 50 µl of gill homogenate was mixed
257 with 50 µl of caspase reagent solution (50µl caspases-3/7 substrate Ac-DEVD-AFC, 200
258 µl of DTT and 4.75 ml of assay buffer) in a black, v-bottom, 96-well plate. Caspase-3/7
259 mediated conversion of the substrate N-acetyl-Asp-Glu-Val-Asp-7 amino-4
260 trifluoromethyl coumarin was monitored every 5 min over a 60 min duration using a
261 TECAN® microplate reader (λ_{ex} : 380 nm, λ_{em} : 500 nm; TECAN Group, Switzerland).
262 The protein concentration of gill tissue homogenates was estimated using the Quick
263 Start™ Bradford 1 x Dye Reagent (BIO-RAD, cat #500-0205) in a microplate format
264 with bovine serum albumin (BSA) as the standard. Caspase-3/7 activity was expressed
265 in Relative Fluorescence Unit per min per mg of protein.

266

267 2.6 Statistical analysis

268 Two-way analysis of variance (ANOVA) was performed to test the affect of the
269 four treatments and five time-points on caspase-3/7 activity and gene expression of *C.*
270 *gigas*/OsHV-1. Tukey's honest significance difference method for multiple comparisons
271 was used to compare means if significant differences were found. Statistical analysis
272 and graphs were produced using the computer package, SPSS version 20.0.0.2.

273

274 3.0 Results

275 3.1 Viral load in gill tissue and oyster cumulative mortality

276 The cumulative mortality of *C. gigas* injected with the OsHV-1 homogenate was
277 $13.4 \pm 5.8\%$. The timing of mortality for *C. gigas* injected with the OsHV-1 homogenate
278 occurred between 54 and 96 h post infection (p.i.). No mortality occurred in *C. gigas*
279 injected with the OsHV-1 homogenate + poly I:C, control homogenate and control
280 homogenate + poly I:C.

281 The concentration of OsHV-1 DNA in gill tissue was quantified for each individual
282 oyster during the experiment. The concentration of OsHV-1 DNA in *C. gigas* gill tissue
283 was below 1.0×10^1 copies per ng of total DNA at 0, 3 and 9 h p.i. for all four treatments
284 (Figure 1). At 27 h, *C. gigas* injected with OsHV-1 homogenate had a mean OsHV-1 DNA
285 concentration of 9.45×10^5 copies per ng of total DNA, which dropped to a mean
286 concentration of 4.06×10^3 copies per ng of total DNA at 54 h. For *C. gigas*

287 simultaneously injected with OsHV-1 + poly I:C, mean concentration of OsHV-1 DNA
288 was 3.15×10^2 copies per ng of total DNA at 27 h and the mean concentration of OsHV-1
289 increased to 1.53×10^3 copies per ng of total DNA at 54 h. The concentration of OsHV-1
290 DNA was less than 1.0×10^1 copies per ng of total DNA for *C. gigas* injected with the
291 control homogenates at all time points (Figure 1).

292

293 3.2 *Crassostrea gigas* gene expression in gill tissue

294 We measured the expression kinetics of 15 *C. gigas* genes in response to OsHV-1
295 infection and poly I:C stimulation. These target genes were involved in the apoptotic
296 pathway (TNF_1, TNF_2, TNF_3, TNFR_1, TNFR_2, IAP_1, IAP_2, caspase 3 & caspase 7),
297 ISG response (PKR, ADAR-L, viperin, CH25H) and host cellular replication (RNR,
298 Helicase_1 & Helicase_2). The expression of those target genes were normalised to
299 elongation factor (eEF1 α), which was stable in the current experiment (CV = 5.1 %, $p =$
300 0.312). At 27 h, the mRNA levels of ISGs (viperin, PKR and ADAR) and TNF3 was
301 significantly elevated in *C. gigas* injected with the OsHV-1 homogenate (Figure 2, $p <$
302 0.001). The mRNA expression levels of these ISGs and TNF3 returned to normal by 54 h
303 ($p > 0.05$). In contrast, only viperin mRNA levels was significantly elevated at 27 h in *C.*
304 *gigas* injected simultaneously with OsHV-1 + poly I:C (Figure 2A, $p < 0.05$). OsHV-1
305 infection did not alter the mRNA expression levels of the other target genes (TNF1,
306 TNF2, TNFR1, TNFR2, IAP1, IAP2, caspase 3 & caspase 7) involved in the apoptotic
307 pathway ($p > 0.05$). Likewise, injection of the control homogenate or control
308 homogenate + poly I:C did not alter the expression levels of any of the target genes
309 investigated ($p > 0.05$).

310

311 3.3 OsHV-1 gene expression in gill tissue

312 OsHV-1 RNA was detected in *C. gigas* gill tissue using RT-qPCR and we report
313 both qualitative and quantitative values for OsHV-1 gene expression. Qualitative
314 detection determines whether a target RNA is present in a sample. We considered a
315 sample to contain OsHV-1 RNA when SYBR fluorescence in the assay exceeded the
316 threshold of 0.1 relative fluorescent units (RFU) within 40 cycles of PCR. We first
317 detected RNA transcripts corresponding to OsHV-1 ORF51 (Ribonuclease Reductase)
318 and ORF67 (Helicase) at 3 h post inoculation (p.i). Whereas, RNA transcripts

319 corresponding to ORF87 (IAP), ORF106 (IAP), ORF57 (CH25H) and ORF115 (Helicase)
320 were not detected by RT-qPCR in gill tissue until 27 hours p.i.

321 OsHV-1 gene expression was also normalised to the number of OsHV-1 DNA
322 genome copies within the gill tissue. Normalisation revealed these six OsHV-1 RNA
323 transcripts were all significantly expressed at 27 h in *C. gigas* inoculated with the OsHV-
324 1 homogenate (Figure 3, $p < 0.05$), but the normalised expression of these six RNA
325 transcripts was significantly lower at 27 h in *C. gigas* simultaneously injected with
326 OsHV-1 + poly I:C (Figure 3, $p > 0.05$).

327

328 3.4 Histopathology and apoptotic cell localisation

329 There were microscopic changes to the epithelium of *C. gigas* injected with
330 OsHV-1 poly at 27 and 54 hours p.i. Examination of the epithelium tissue of *C. gigas*
331 injected with the OsHV-1 homogenate and OsHV-1 homogenate + poly I:C revealed
332 multifocal erosive lesions with underlying hemocyte infiltration at 27 and 54 h p.i.
333 (Figure 4A). These changes were not observed in *C. gigas* injected with the control
334 homogenate or control homogenate + poly I:C (Figure 4B).

335 *In-situ* detection of fragmented DNA (TUNEL assay) was undertaken to identify
336 apoptotic cells in oyster tissues. The positive control (DNase I treated) showed
337 extensive staining in all nuclei examined (data not shown). The TUNEL assay revealed
338 apoptotic cells in *C. gigas* injected with both the OsHV-1 and control homogenates. We
339 did not observe a focal accumulation of apoptotic cells in any tissue type that was
340 specific to oysters injected with the OsHV-1 homogenate.

341

342 3.5 Caspase-3/7 activity

343 OsHV-1 and poly I:C did not alter the activity of caspase-3/7 at 0, 27 and 54 h
344 post injection ($p > 0.05$, Figure 5).

345

346 4.0 Discussion

347 Vertebrates and model-invertebrates have evolved effective anti-viral responses
348 [1]. The RNAi machinery can inhibit virus replication [49], whereas other evolutionary
349 conserved anti-viral responses, such as apoptosis and the IFN-pathway, are capable of
350 clearing viruses from the host [12, 50]. In order for viruses to replicate and propagate,
351 viruses also evolved strategies to counteract the host anti-viral response [36]. The first

352 objective of this study was to investigate OsHV-1 countermeasure to the oyster's anti-
353 viral response involving apoptosis and ISG expression. These two anti-viral pathways
354 were chosen based on OsHV-1 ORFs that shared high homology to *C. gigas* inhibitors of
355 apoptosis and CH25H. We also investigated OsHV-1 ORFs that share high homology to
356 *C. gigas* genes involved in DNA metabolism.

357 In the current study, OsHV-1 was confirmed to replicate in the gill tissue of *C.*
358 *gigas* upon infection. The amount of OsHV-1 DNA in gill tissue of *C. gigas* injected with
359 the OsHV-1 homogenate was below the quantifiable lower limit at 0, 3 and 9 h p.i. and
360 then rapidly increased to peak at 27 h p.i. (Figure 1). This pattern of OsHV-1 replication
361 is similar to previous studies investigating OsHV-1 replication in mantle tissue [44-46],
362 however these studies first detected OsHV-1 DNA at 2 h p.i. OsHV-1 DNA was detected
363 in some control oyster samples in the present study, but the amount of DNA was below
364 the quantifiable lower limit. The presence of OsHV-1 DNA in control animals is a
365 recurrent problem [40, 44, 51] and may represent contamination or a persistent/latent
366 infection. However, OsHV-1 was not causing an active infection in control oysters
367 because we failed to detect OsHV-1 RNA by RT-qPCR (Section 3.3). OsHV-1 mRNA
368 corresponding to genes involved in DNA metabolism (ORF51 and ORF67) were first
369 detected by RT-qPCR in the OsHV-1 treatment at 3 h post-infection and OsHV-1 mRNA
370 corresponding to genes (ORF57, ORF87 and ORF106) that potentially modulate the
371 host's immune response were not detected until 27 h post-infection. This pattern of
372 OsHV-1 gene expression is similar to previous studies using *C. gigas* mantle tissue [45].
373 The corresponding *C. gigas* genes involved in DNA metabolism (ribonuclease reductase
374 and DNA helicases), inhibitors of apoptosis (IAPs) and CH25H remained stable in
375 response to OsHV-1 infection.

376 Apoptosis is an important process to eliminate virus-infected cells that pose a
377 threat to the host [50]. Electron microscopic examination of *C. gigas* larvae and spat
378 infected with OsHV-1 revealed hemocytes with condensed chromatin and extensive
379 perinuclear fragmentation of chromatin, which suggest OsHV-1 may induce apoptosis in
380 oyster hemocytes [52]. The process of apoptosis is evolutionary conserved [53, 54] and
381 regulated by a specific set of genes [50]. Apoptotic signals are initiated and transduced
382 via intrinsic (mitochondrial-mediated) or extrinsic (immune-mediated) pathways [50].
383 Extracellular signals can activate the extrinsic pathway through death receptors,
384 resulting in the recruitment of FADD and caspase-8 and forming the death-inducing

385 signalling complex (DISC) [55]. Activated caspase-8 then activates caspase-3, which
386 plays a central role in the execution phase of apoptosis [55]. Ligands that activate the
387 death receptors belong to the TNF superfamily of cytokines [55]. In the current study,
388 we measured the mRNA expression levels of three TNF cytokines and two TNF-
389 receptors in gill tissue of *C. gigas*. OsHV-1 infection resulted in the up-regulation of a
390 single TNF (GenBank #ADX31292, Figure 2) at 27 h post-infection, but we did not
391 observe evidence that apoptosis was induced in response to OsHV-1 infection. We
392 assessed apoptosis using three independent assays: biochemical assay to measure
393 caspase-3,7 activity (Figure 5), TUNEL reaction to localise apoptotic cells in histology
394 sections and a molecular assay to measure gene expression of caspase 3 and 7 (Figure
395 2). Some viruses have evolved distinct strategies to evade apoptosis to facilitate
396 replication, spread and latency [50]. The genomes of mammalian herpesviruses encode
397 immunomodulators that have host counterparts [reviewed by 50]. For example,
398 Epstein-Barr virus (EBV) encodes an IAP (BHRF1) in the early stages of infection to
399 prevent TNF α -induced apoptosis [56]. OsHV-1 also encodes four IAPs with high
400 homology to *C. gigas* IAPs (Table 1). In the current study, two OsHV-1 IAPs (ORF87 &
401 ORF106) were significantly up-regulated at 27 h post-infection (Figure 3), suggesting
402 OsHV-1 IAPs might play an important role in OsHV-1 replication via protecting infected
403 *C. gigas* cells from TNF-mediated apoptosis, thus maximising viral particle numbers in
404 the early stages of infection. Previous studies have also reported that OsHV-1 ORF87 is
405 expressed during the early stages (10 h p.i.) of OsHV-1 infection [44-46].

406 Previous research has demonstrated that *C. gigas* injected with a high
407 concentration of dsRNA (poly I:C, 5 mg.ml⁻¹) have elevated mRNA expression levels of
408 ISGs at 27 h post-injection [24, 25] and these oysters are resistant to subsequent
409 infection with OsHV-1 [22]. In the current experiment, *C. gigas* were injected with a
410 lower concentration of poly I:C (1 mg.ml⁻¹) and this concentration of poly I:C was
411 insufficient to induce ISG expression (Figure 2). We observed *C. gigas* injected with a
412 low concentration of poly I:C (OsHV-1 homogenate + poly I:C) are still capable of
413 inhibiting both OsHV-1 replication (Figure 1) and OsHV-1 gene expression (Figure 3)
414 compared to *C. gigas* injected with only the OsHV-1 homogenate. These observations
415 suggest non-specific dsRNA induces both an ISG response and an additional anti-viral
416 pathway in *C. gigas*. In other animal models, dsRNA not only activates the interferon-
417 response, but it is also known to regulate different types of post-transcription gene

418 processes that are collectively referred to as RNA interference (RNAi) [57]. RNAi can
419 silence virus gene expression (virus-derived short interfering RNAs) [57]. The RNAi
420 system is functional in oysters [reviewed by 58, 59], but the contribution of RNAi to
421 oyster anti-viral immunity is unknown. Research from other marine invertebrates
422 suggests there is cross-talk between the RNAi-mediated anti-viral pathway and the
423 transcriptomic response induced by non-specific dsRNA [60, 61].

424 In the current study we observed a reduction in the concentration of OsHV-1
425 DNA between 27 and 54 h p.i. (Figure 1), which suggests *C. gigas* may have a mechanism
426 to clear OsHV-1 from infected gill tissue. From our data, we speculate on two potential
427 mechanisms to clear OsHV-1 from infected gill cells. The multifocal erosive lesions of
428 epithelium tissue could be a host response to shed virus-infected gill cells (Figure 4).
429 These histological observations are consistent with previous studies [62, 63].
430 Cytopathological changes of scallop, *Chlamyl farreri* infected with acute virus
431 necrobiotic virus (AVNV, genotype of OsHV-1) include focal erosive lesions of
432 epithelium cells and these cells were positive for AVNV using *in-situ* immunofluorescent
433 detection and monoclonal antibodies raised against AVNV [63]. However, *in-situ*
434 hybridisation of *C. gigas* reveals OsHV-1 DNA is mainly observed in connective tissue of
435 mantle, gills, adductor muscle, labial palps and gonads [40, 64] and we observed
436 epithelium lesions in *C. gigas* injected with OsHV-1 homogenate + poly I:C, but no
437 reduction in the concentration of OsHV-1 DNA in this group of *C. gigas* between 27 and
438 54 h p.i. (Figure 1). The more likely alternative mechanism for *C. gigas* to clear OsHV-1
439 from infected gill tissue is the up-regulation of ISGs (*i.e.* viperin, PKR, ADAR) at 27 h p.i.
440 (Figure 2). In support of this mechanism is the lack of ISG induction in *C. gigas*
441 simultaneously injected with OsHV-1 homogenate + poly I:C (Figure 2) corresponding
442 with no change in OsHV-1 DNA concentration in gill tissue between 27 and 54 h p.i.
443 (Figure 1).

444

445 **Conclusion**

446 Results from our study support the concept that IAPs encoded by the OsHV-1 genome
447 can successfully inhibit apoptosis in gill tissue of *C. gigas*. If experimental infection of *C.*
448 *gigas* with OsHV-1 resulted in the initiation of the extrinsic apoptotic pathway (TNF₃
449 up-regulation), we didn't observe evidence of apoptosis using a combination of
450 biochemical and molecular assays. Interestingly, we observed evidence that dsRNA

451 induces an additional antiviral response in *C. gigas* that is capable of inhibiting OsHV-1
452 replication. Future research should focus on characterising the RNAi-mediated antiviral
453 pathway in response to OsHV-1 infection and examine if cross-talk occurs between the
454 IFN-like and RNAi response in *C. gigas*.

455

456 **Acknowledgements**

457 The authors acknowledge the funding provided to T. Green by Macquarie University
458 Research Fellowship Scheme (MQ Grant: 9201300681). The authors are grateful to
459 Bruno Petton and Ifremer's Argenton facility staff for production of spat (Ifremer FINA
460 action) and Max Nourry and Ifremer's Bouin facility staff for taking care and dispatch of
461 spat between Ifremer's laboratories.

462

463 **5.0 References**

464

- 465 1. Loker ES, Adema CM, Zhang S-M, Kepler TB. Invertebrate immune systems - not
466 homogeneous, not simple, not well understood. *Immunolog Rev.* 2004 198:10-24.
- 467 2. Green TJ, Raftos DA, Speck P, Montagnani C. Antiviral immunity in marine
468 molluscs. *J Gen Virol.* 2015 Epub ahead of print.
- 469 3. Fragkoudis R, Attarzadeh-Yazdi G, A.A. N, Fazakerley JK, Kohl A. Advances in
470 dissecting mosquito innate immune responses to arbovirus infection. *J Gen Virol.* 2009
471 90:2061-72.
- 472 4. Blair CD. Mosquito RNAi is the major innate immune pathway controlling
473 arbovirus infection and transmission. *Future Microbiol.* 2011 6:265-77.
- 474 5. Lamiable O, Imler J-L. Induced antiviral innate immunity in *Drosophila*. *Curr Opin*
475 *Immunol.* 2014 20:62-8.
- 476 6. Wilkins C, Dishongh R, Moore SC, Whitt MA, Chow M, Machaca K. RNA
477 interference is an antiviral defence mechanism in *Caenorhabditis elegans*. *Nature.* 2005
478 436:1044-7.
- 479 7. Kemp C, Mueller S, Goto A, Barbier V, Paro S, Bonnay F, et al. Broad RNA
480 interference-mediated antiviral immunity and virus-specific inducible responses in
481 *Drosophila*. *J Immunol.* 2013 190:650-8.
- 482 8. Nakamoto M, Moy RH, Xu J, Bambina S, Yasunaga A, Shelly SS, et al. Virus
483 recognition by Toll-7 activates antiviral autophagy in *Drosophila*. *Immunity.* 2012
484 36:658-67.
- 485 9. Dostert C, Jouanguy E, Irving P, Troxler L, Galiana-Arnoux D, Hetru C, et al. The
486 Jak-STAT signaling pathway is required but not sufficient for the antiviral response of
487 *drosophila*. *Nat Immunol.* 2005 6:946-53.
- 488 10. Xi Z, Ramirez JL, Dimopoulos G. The *Aedes aegypti* Toll pathway controls dengue
489 virus infection. *Plos Pathogens.* 2008 4:e1000098.
- 490 11. Jeang K-T. RNAi in the regulation of mammalian viral infections. *BMC Biol.* 2012
491 10:58-63.

- 492 12. Randall RE, Goodbourn S. Interferons and viruses: an interplay between
493 induction, signalling, antiviral responses and viral countermeasures. *J Gen Virol.* 2008
494 89:1-47.
- 495 13. Schoggins JW, Rice CM. Interferon-stimulated genes and their antiviral effector
496 functions. *Curr Opin Virol.* 2011 1:519-25.
- 497 14. Robalino J, Browdy CL, Prior S, Metz A, Parnell P, Gross PS, et al. Induction of
498 antiviral immunity by double-stranded RNA in a marine invertebrate. *J Virol.* 2004
499 78:10442-8.
- 500 15. He Y, Jouaux A, Ford SE, Lelong C, Sourdain P, Mathieu M, et al. Transcriptome
501 analysis reveals strong and complex antiviral response in a mollusc. *Fish Shellfish*
502 *Immunol.* 2015 46:131-44.
- 503 16. Garrison K, Hernandez A. Progress in using coral as a model to study intrinsic
504 and innate immune responses to herpes-like viruses. *The Journal of Immunology.* 2014
505 192:207.4.
- 506 17. Kuusksalu A, Subbi J, Pehk T, Reintamm T, Muller WEG, Kelve M. Identification of
507 the reaction products of (2'-5')oligoadenylate synthetase in the marine sponge. *Eur J*
508 *Biochem.* 1998 257:420-6.
- 509 18. Schröder HC, Natalio F, Wiens M, Tahir MN, Shukoor MI, Tremel W, et al. The 2'-
510 5'-oligoadenylate synthetase in the lowest metazoa: isolation, cloning, expression and
511 functional activity in the sponge *Lubomirskia baicalensis*. *Mol Immunol.* 2008 45:945-
512 53.
- 513 19. Kortschak DR, Samuel G, Saint R, Miller DJ. EST analysis of the Cnidarian
514 *Acropora millepora* reveals extensive gene loss and rapid sequence divergence in the
515 model invertebrates. *Curr Biol.* 2003 13:2190-5.
- 516 20. Miller DJ, Hemmrich G, Ball EE, Haywar DC, Khalturin K, Funayama N, et al. The
517 innate immune repertoire in Cnidaria - ancestral complexity and stochastic gene loss.
518 *Genome Biol.* 2007 8.
- 519 21. Rosani U, Varotto L, Domeneghetti S, Arcangeli G, Pallavicini A, Venier P. Dual
520 analysis of host and pathogen transcriptomes in Ostreid herpesvirus 1 - positive
521 *Crassostrea gigas*. *Environ Microbiol.* In Press:DOI: 10.1111/462-2920.12706.
- 522 22. Green TJ, Montagnani C. Poly I:C induces a protective antiviral immune response
523 in the Pacific oyster (*Crassostrea gigas*) against subsequent challenge with Ostreid
524 *herpesvirus* (OsHV-1 μ var). *Fish Shellfish Immunol.* 2013 35:382-8.
- 525 23. Renault T, Faury N, Barbosa-Solomieu V, Moreau K. Suppression subtractive
526 hybridisation (SSH) and real time PCR reveal differential gene expression in the Pacific
527 cupped oyster, *Crassostrea gigas*, challenged with Ostreid herpesvirus 1. *Dev Comp*
528 *Immunol.* 2011 35:725-35.
- 529 24. Green TJ, Benkendorff K, Robinson N, Raftos D, Speck P. Anti-viral gene induction
530 is absent upon secondary challenge with double-stranded RNA in the Pacific oyster,
531 *Crassostrea gigas*. *Fish Shellfish Immunol.* 2014 39:492-7.
- 532 25. Green TJ, Montagnani C, Benkendorff K, Robinson N, Speck P. Ontogeny and
533 water temperature influences the antiviral response of the Pacific oyster, *Crassostrea*
534 *gigas*. *Fish Shellfish Immunol.* 2014 36:151-7.
- 535 26. Moreau P, Moreau K, Segarra A, Tourbiez D, Travers M-A, Rubinsztein DC, et al.
536 Autophagy plays an important role in protecting Pacific oysters from OsHV-1 and *Vibrio*
537 *aestuarianus* infections. *Autophagy.* 2015 In Press.
- 538 27. Segarra A, Pepin JF, Arzul I, Morga B, Faury N, Renault T. Detection and
539 description of a particular Ostreid herpesvirus 1 genotype associated with massive

- 540 mortality outbreaks of Pacific oysters, *Crassostrea gigas*, in France in 2008. Virus Res.
541 2010 153:92-9.
- 542 28. Ren W, Chen H, Renault T, Cai Y, Bai C, Wang C. Complete genome sequence of
543 acute viral necrosis virus associated with massive mortality outbreaks in the Chinese
544 scallop, *Chlamys farreri*. Virol J. 2013 10:110.
- 545 29. Crane MSJ, Corbeil S, Williams LM, McColl KA, Gannon V. Evaluation of abalone
546 viral ganglioneuritis resistance among wild abalone populations along the Victorian
547 coast of Australia. J Shellfish Res. 2013 32:67-72.
- 548 30. Hooper C, Hardy-Smith P, Handlinger J. Ganglioneuritis causing high mortalities
549 in farmed Australian abalone (*Haliotis laevis* and *Haliotis rubra*). Aust Vet J. 2007
550 85:188-93.
- 551 31. Davison AJ, Eberia R, Ehlers B, Hayward GS, McGeoch DJ, Minson AC, et al. The
552 order *Herpesvirales*. Arch Virol. 2009 154:171-7.
- 553 32. Savin KW, Cocks BG, Wong FYK, Sawbridge T, Cogan N, Savage D, et al. A
554 neurotropic herpesvirus infecting the gastropod, abalone, shares ancestry with oyster
555 herpesvirus and a herpesvirus associated with the amphioxus genome. Virology Journal.
556 2010 7:308-.
- 557 33. Davison AJ, Trus BL, Cheng N, Steven AC, Watson MS, Cunningham C, et al. A
558 novel class of herpesvirus with bivalve hosts. J Gen Virol. 2005 86:41-53.
- 559 34. Areste C, Blackbourn DJ. Modulation of the immune system by Kaposi's sarcoma-
560 associated herpesvirus. Trends Microbiol. 2009 17:119-29.
- 561 35. White DW, Beard SR, Barton ES. Immune modulation during latent herpesvirus
562 infection. Immunol Rev. 2012 245:189-208.
- 563 36. Vandevienne P, Sadzot-Delvaux C, Piette J. Innate immune response and viral
564 interference strategies developed by Human Herpesviruses. Biochem Pharm. 2010
565 80:1955-72.
- 566 37. Liu S-Y, Aliyari R, Chikere K, Li G, Marsden MD, Smith JK, et al. Interferon-
567 inducible cholesterol-25-hydroxylase broadly inhibits viral entry by production of 25-
568 hydroxycholesterol. Immunity. 2013 38:92-105.
- 569 38. Weller SK, Coen DM. Herpes Simplex Viruses: Mechanisms of DNA replication.
570 Cold Spring Harb Perspect Biol. 2012 4:a013011.
- 571 39. Schikorski D, Renault T, Saulnier D, Faury N, Moreau P, Pepin JF. Experimental
572 infection of Pacific oyster *Crassostrea gigas* spat by ostreid herpesvirus 1:
573 demonstration of oyster spat susceptibility. Vet Res. 2011 42:27.
- 574 40. Corbeil S, Faury N, Segarra A, Renault T. Development of an *in situ* hybridization
575 assay for the detection of ostreid herpesvirus type 1 mRNAs in the Pacific oyster,
576 *Crassostrea gigas*. J Virol Methods. 2015 211:43-50.
- 577 41. Cadoret K, Bridle AR, Leef MJ, Nowak BF. Evaluation of fixation methods for
578 demonstration of *Neoparamoeba perurans* infection in Atlantic salmon, *Salmo salar* L.,
579 gills. J Fish Dis. 2013 2013:831-9.
- 580 42. Pepin JF, Riou A, Renault T. Rapid and sensitive detection of ostreid herpesvirus
581 1 in oyster samples by real-time PCR. J Virol Methods. 2008 149:269-76.
- 582 43. de Lorgeril J, Zenagui R, Rosa R, Piquemal D, Bachere E. Whole transcriptome
583 profiling of successful immune response to *Vibrio* infections in the oyster *Crassostrea*
584 *gigas* by digital gene expression analysis. Plos One. 2011 6:e23142.
- 585 44. Segarra A, Baillon L, Tourbiez D, Benabdelmouna A, Faury N, Bourgougnon N, et
586 al. Ostreid herpesvirus type 1 replication and host response in adult Pacific oysters,
587 *Crassostrea gigas*. Vet Res. 2014 45.

- 588 45. Segarra A, Faury N, Pepin J-F, Renault T. Transcriptomic study of 39 ostreid
589 herpesvirus 1 genes during an experimental infection. *J Invert Pathol.* 2014 119:5-11.
- 590 46. Segarra A, Mauduit F, Faury N, Trancart S, D'egremont L, Tourbiez D, et al. Dual
591 transcriptomics of virus-host interactions: comparing two Pacific oyster families
592 presenting contrasted susceptibility to ostreid herpesvirus 1. *BMC Genomics.* 2014
593 15:580-92.
- 594 47. Burge CA, Friedman CS. Quantifying ostreid herpesvirus (OsHV-1) genome
595 copies and expression during transmission. *Microb Ecol.* 2012.
- 596 48. Rolland J-L, Medhioub W, Vergnes A, Abi-khalil C, Savar V, Abadie E, et al. A
597 feedback mechanism to control apoptosis occurs in the digestive gland of the oyster
598 *Crassostrea gigas* exposed to the paralytic shellfish toxins producer *Alexandrium*
599 *catenella*. *Mar Drugs.* 2014 12:5035-54.
- 600 49. Berkhout B, Haasnoot J. The interplay between virus infection and the cellular
601 RNA interference machinery. *FEBS Letters.* 2006 580:2896-902.
- 602 50. Quinian MP. Apoptosis and virus infection. In: Granoff A, Webster RG, editors.
603 *Encyclopedia of Virology: Elsevier Ltd; 1999*, p. 68-76.
- 604 51. Whittington RJ, Paul HM, Evans O, Rubio A, Alford B, Dhand N, et al. Protection of
605 Pacific oyster (*Crassostrea gigas*) spat from mortality due to Ostreid herpes virus-1
606 (OsHV-1 uvar) using simple treatments of incoming seawater in land-based upwellers.
607 *Aquaculture.* 2015 437:10-20.
- 608 52. Renault T, Le Deuff R-M, Chollet B, Cochenec N, Gerard A. Concomitant herpes-
609 like virus infections in hatchery-reared larvae and nursery-cultured spat *Crassostrea*
610 *gigas* and *Ostrea edulis*. *Dis Aquat Org.* 2000 42:173-83.
- 611 53. Quistad SD, Stotland A, Barott KL, Smurthwaite CA, Jameson Hilton B, Grasis JA,
612 et al. Evolution of TNF-induced apoptosis reveals 550 My of functional conservation.
613 *Proc Natl Acad Sci USA.* 2014 111:9567-72.
- 614 54. Zhang L, Li L, Zhang G. Gene discovery, comparative analysis and expression
615 profile reveal the complexity of the *Crassostrea gigas* apoptosis system. *Dev Comp*
616 *Immunol.* 2011 35:603-10.
- 617 55. Degtarev A, Yuan J. Expansion and evolution of cell death programmes. *Nat Rev*
618 *Mol Cell Biol.* 2008 9:378-90.
- 619 56. Kawanishi M. Epstein-Barr virus BHRF1 protein protects intestine 407 epithelial
620 cells from apoptosis induced by tumor necrosis factor alpha and anti-Fas antibody. *J*
621 *Virol.* 1997 71:3319-22.
- 622 57. Meister G, Tuschli T. Mechanisms of gene silencing by double-stranded RNA.
623 *Nature.* 2004 431:343-9.
- 624 58. Lima PC, Harris JO, Cook M. Exploring RNAi as a therapeutic strategy for
625 controlling disease in aquaculture. *Fish Shellfish Immunol.* 2013 34:729-43.
- 626 59. Owens L, Malham S. Review of the RNA interference pathway in molluscs
627 including some possibilities for use in bivalve aquaculture. *J Mar Sci Eng.* 2015 3:87-99.
- 628 60. Robalino J, Bartlett T, Shepard E, Prior S, Jaramillo G, Scura E, et al. Double-
629 stranded RNA induces sequence-specific antiviral silencing in addition to non-specific
630 immunity in a marine shrimp: convergence of RNA interference and innate immunity in
631 the invertebrate antiviral response? *J Virol.* 2005 79:13561-71.
- 632 61. Labreuche Y, Veloso A, de la Vega E, Gross PS, Chapman RW, Browdy CL, et al.
633 Non-specific activation of antiviral immunity and induction of RNA interference may
634 engage the same pathway in the Pacific white leg shrimp *Litopenaeus vannamei*. *Dev*
635 *Comp Immunol.* 2010 34:1209-18.

- 636 62. Jenkins C, Hick P, Gabor M, Spiers Z, Fell SA, Gu X, et al. Identification and
637 characterisation of an ostreid herpesvirus-1 microvariant (OsHV-1 u-var) in *Crassostrea*
638 *gigas* (Pacific oysters) in Australia. *Dis Aquat Org.* 2013 105:109-26.
- 639 63. Fu C, Song L, Li Y. Monoclonal antibodies developed for detection of an epizootic
640 virus associated with mass mortalities of cultured scallop *Chlamys farreri*. *Dis Aquat*
641 *Org.* 2005 65:17-22.
- 642 64. Arzul I, Renault T, Thebault A, Gerard A. Detection of oyster herpesvirus DNA
643 and proteins in asymptomatic *Crassostrea gigas* adults. *Virus Res.* 2002 84:151-60.
644
645

646 Table and Figure Legends

647 Table 1: Quantitative PCR primers used for measuring *Crassostrea gigas* and OsHV-1
648 gene expression. The E-value and amino acid identify (Identity %) are provided for
649 OsHV-1 ORFs that are homologous to *C. gigas* genes.

650

651 Figure 1: Absolute quantification of OsHV-1 DNA in gill tissue of *Crassostrea gigas* by
652 quantitative PCR according to Pepin and Renault et al [42].

653

654 Figure 2: Normalised gene expression of selected *Crassostrea gigas* immune genes
655 (mean \pm SD). Among the 15 *C. gigas* target genes that were investigated, only four genes
656 were differentially upregulated following OsHV-1 infection, viperin (A), PKR (B), ADAR
657 (C) and TNF3 (D). The expression of *C. gigas* caspase-3 (E) and caspase-7 (F) were not
658 up-regulated following OsHV-1 infection or poly I:C injection ($p > 0.05$). Different letters
659 indicate significant differences between treatments and time-points ($p < 0.05$, Tukey's
660 HD).

661

662 Figure 3: Normalised viral gene expression of selected OsHV-1 open reading frames
663 (ORFs). The expression of OsHV-1 ORFs were normalised according to Segarra et al,
664 [44] and their expression (mean \pm SD) is present in individual graphs: (A) ORF51, (B)
665 ORF57, (C) ORF87, (D) ORF106, (E) ORF67, and (F) ORF115.. Asterisks indicate the ORF
666 was significant up-regulated ($p < 0.05$, Tukey's HD).

667

668 Figure 4: OsHV-1 infection of *Crassostrea gigas* was associated with multifocal
669 ulceration the mantle and gill epidermis (arrows) with underlying inflammation (*) at
670 27 and 54 hour post-injection. (A) Mantle epithelium of *C. gigas* injected with OsHV-1
671 homogenate at 27 h p.i. (B) Mantle epithelium of *C. gigas* injected with control
672 homogenate at 27 h post-injection. Scale bar corresponds to 100 μ m is indicated.

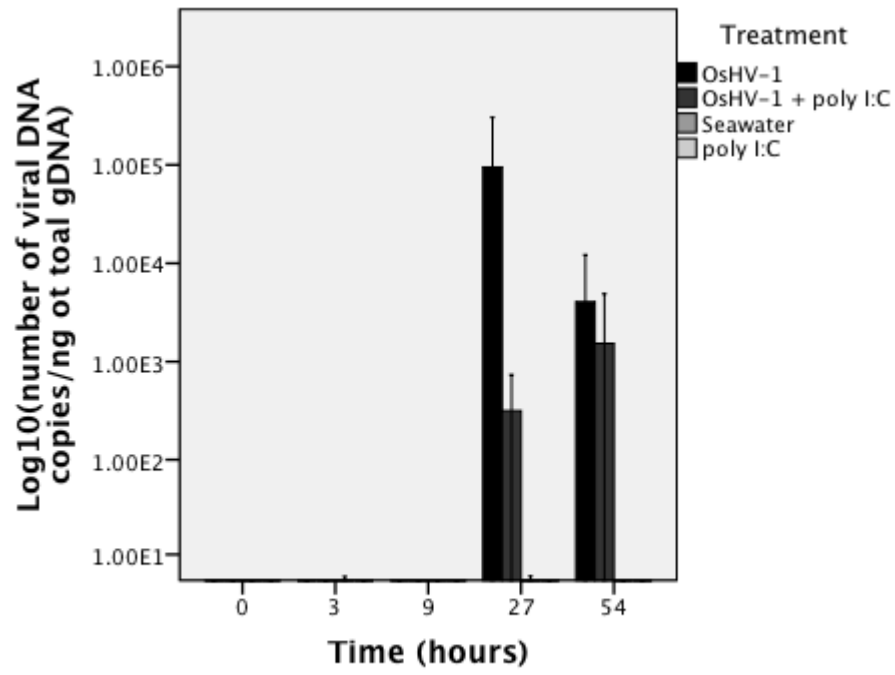
673

674 Figure 5: Caspase-3/7 activity measurements in the gill tissue of *Crassostrea gigas* at 0,
675 27 and 54 h post-injection (mean \pm SD). OsHV-1 infection or poly I:C injection did not
676 alter the activity of caspase-3/7 (two-way ANOVA, $p > 0.05$).

677 **Table 1**

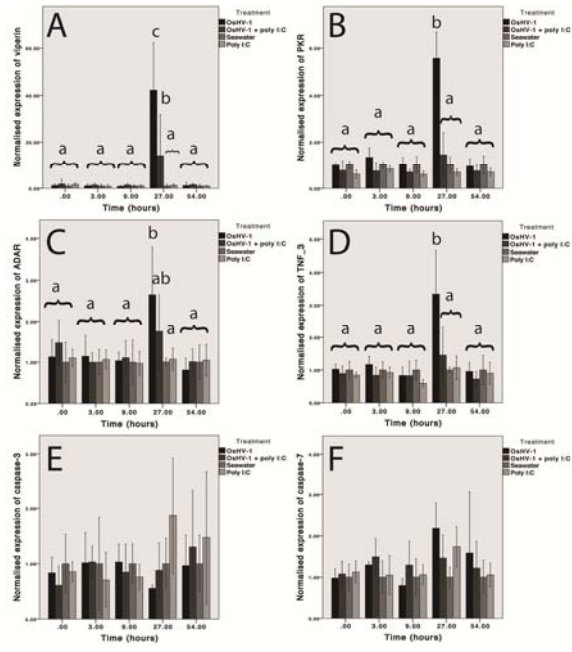
Function	Gene	Host (<i>Crassostrea gigas</i>)			Virus (OsHV-1)				%Identity	E-value
		Genbank	5'	3'	ORF	Genbank	5'	3'		
Reference	EFU	ABI22066	GAGCGTGAACGTGGTATCAC	ACAGCACAGTCAGCCTGTGA						
Apoptosis	TNF1	EKC35160	ACCCGGTAGCTCACATAC	ACGTAGTGATACAGCGTTGTAG						
Apoptosis	TNF2	EKC39243	CTGGATTTACGACAGAGACATC	ACGACACCTGGCTGTAGAC						
Apoptosis	TNF_3	ADX31292	ATCTACCACCAACGTGCAAC	GTCTTAAGGTCGGATTGGAG						
Apoptosis	TNFR_1	EKC31251	TATCGTCGCCGCCATCATC	TGACCTTGAATGACCCTGAC						
Apoptosis	TNFR_2	EKC31251	TATCGTCGCCGCCATCATC	TGACCTTGAATGACCCTGAC						
Apoptosis	Caspase-3	CU988427	ATCACCAGGAAGGATCATGG	GTTTCATCCGAACACGACTCG						
Apoptosis	Caspase-7	HQ425703	ATTGGACCACAGAGACAACG	TGTTGCCTTTGAAGGGCTCC						
Apoptosis	IAP_1	EKC36433	CATCTTCTTCTCATCGGCTTC	TCAGCTGTTGAGGTGTGAC	ORF87	Q6R7E2	CACAGACGACATTTCCCAAA	AAAGCTCGTTCACATTGGT	36	8.E-47
Apoptosis	IAP_2	EKC34022	CAGTAAAGAGGCCAGCTAG	CTTACTGCTAGGATAGCGTATG	ORF106	Q6R7C4	TCTGGCATCCAACCTCCAAA	TCAGCCTATGACGAGGCAATG	31	2.E-22
ISG	CH25H	EKC31751	CTTTATTGAAATGGGACCCGAAG	GCTATTTTCTGCATGTGAAC	ORF57	Q6R7G8	TTACCAGCACCAGCAGGAT	TGCCCGCTTTTATCCAACAC	20	4.E-15
ISG	Viperin	EKC28205	TAAATGCGGCTTCTGTTTCC	CAGCTGAAGGTCTCTTTGC						
ISG	PKR	EKC34807	GAGCATCAGCAAAGTGTGAG	GTAGCACCAGGAGATGGTTC						
ISG	ADAR-L	EKC20855	CTCAAACAGTGCAACTGCATC	TCACAAGCCCTGCTATCAC						
DNA Metab.	RNR	EKC28390	TGAATCCATAGAGGCATACAC	TCATGTCATCGTCCACAATC	ORF51	Q6R7H4	ACTAACGCAAATGGTAGCCAG	ATCGTGCAGTATTGCGACAC	37	1.E-147
DNA Metab.	Helicase_1	EKC17722	GTCCTGTCCAATCCAAGTC	CTTGATTGTCGTCCGTGAC	ORF67	Q6R7G1	GATGACGGCATTGGTGAGGT	CCTGTGTTGCGGCTTGTTA	23	2.E-16
DNA Metab.	Helicase_2	EKC17722			ORF115	Q6R7B1	ACCACTAAGGCCTTCCAG	GTACAACCTCTGCTGTTTGAC	31	7.E-32

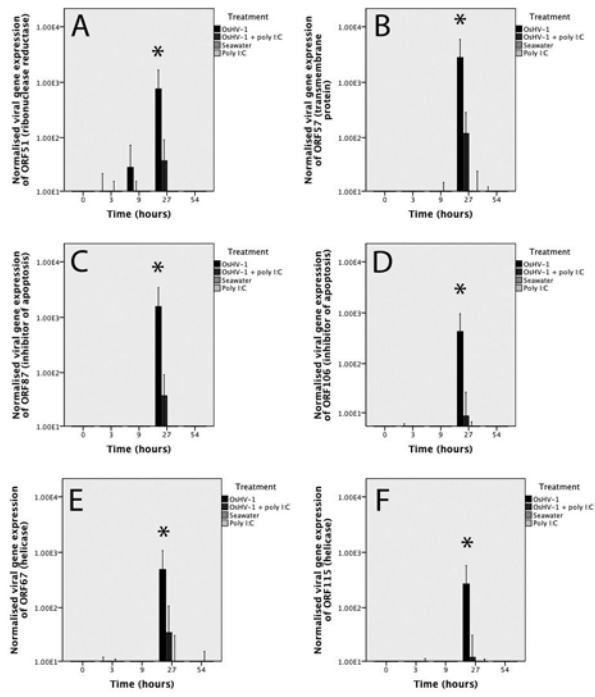
678

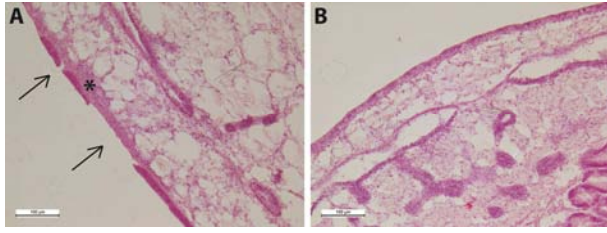


ACCEPTED MANUSCRIPT

ACCEPTED MANUSCRIPT







ACCEPTED MANUSCRIPT

